Clinical Chemistry 51:7
1165–1176 (2005)

Proteomics and
Protein Markers

Development of a High-Throughput Automated Analyzer Using Biochip Array Technology

Stephen P. FitzGerald, John V. Lamont,* Robert I. McConnell, and El O. Benchikh

Background: **Use of protein array technology over conventional assay methods has advantages that include simultaneous detection of multiple analytes, reduction in sample and reagent volumes, and high output of test results. The susceptibility of ligands to denaturation, however, has impeded production of a stable, reproducible biochip platform, limiting most array assays to manual or, at most, semiautomated processing techniques. Such limitations may be overcome by novel biochip fabrication procedures.**

Methods: **After selection of a suitable biochip substrate, biochip surfaces were chemically modified and assessed to enable optimization of biochip fabrication procedures for different test panels. The assay procedure was then automated on a dedicated instrument, and assay performance was determined for a panel of cytokine markers. Assay results were then compared with a commercial method for measurement of cytokine markers.**

Results: **Secondary ion mass spectrometry and x-ray photoelectron spectroscopy demonstrated appropriate and reproducible modification of the biochip surface. Contact-angle studies also confirmed generation of hydrophobic surfaces that enabled containment of droplets for fabrication of discrete test regions. Automation of the biochip assays on a dedicated instrument produced excellent cytokine marker performance with intra- and interassay imprecision <10% for most analytes. Comparison studies showed good agreement with other methods (r = 0.95–0.99) for cytokines.**

Conclusion: **Performance data from this automated biochip array analyzer provide evidence that it is now possible to produce stable and reproducible biochips for output of more than 2000 test results per hour.**

Randox Laboratories, Crumlin, United Kingdom.

*Address correspondence to this author at: Randox Laboratories, 55 Diamond Rd., Crumlin, County Antrim, BT29 4QY United Kingdom. Fax 44-2894-452912; e-mail john.lamont@randox.com.

Received February 14, 2005; accepted April 19, 2005.
Previously published online at DOI: 10.1373/clinchem.2005.049429

Nanotechnology promises new and revolutionary healthcare products, but cost-effective application of nanotechnology to product development and improvement has been challenging *(1)*. Nanotechnology applications for clinical biomarker detection have been documented in the literature *(2)*.

Biomarker detection and quantification can be performed by many available assays, some of which use protein microarray nanotechnology for the fabrication of biochips and the dispensation of nanoliter quantities of ligand solutions on the biochip surface. These microarrays can simultaneously analyze several markers, and their usefulness has been demonstrated in principle *(3, 4)*. Performance has been only moderately productive, however, and commercialization of protein arrays on a biochip platform has been impeded by array construction complexity attributable to the susceptibility of ligands to denaturation. Other confounding factors are related to surface chemistry, antibody binding, labeling, detection, and stabilization. This report describes some of the technical challenges overcome during the development of a new automated system using biochip array technology.

The concept of microarray-based ligand-binding assays was introduced by Ekins et al. *(5–7)* in the late 1980s, and later antibody arrays consisting of 96 wells with 144 elements were constructed for standard ELISAs *(8)*. One advantage of the microarray format is the use of a solid support, which enables the precise deposition of capture molecules in an ordered arrangement on a preactivated surface.

Surface activation techniques include silanation methods, which are simple and cost-effective and have a signal-to-noise ratio that is 3 to 4 times better than other derivatized surfaces *(9)*. Other activation methods include photolithography using light directed spatially through a photomask to modify the array surface at specified locations for ligand attachment. A noncontact approach to ligand deposition on the substrate uses piezoelectric tips for accurate dispensation of capture molecules on the array surface in picoliter to nanoliter quantities. Other array fabrication techniques involve direct array surface contact with solid or split pins.

Studies have revealed that surface chemistry has an effect not only on the binding capacity of the surface but also on activity and stability of the resulting protein layer *(10–12)*. Variations in protein size *(9)*, structure, and charge may affect the performance of the array on different surfaces; therefore, detailed investigation of surface chemistries is required to optimize the ligand attachment process. Spot uniformity is important for microarray fabrication and is determined by the type of surface (hydrophobic or hydrophilic) and the spotting buffer composition *(13)*. Ligand attachment by covalent binding to the surface has been reported to be the most robust approach for antibodies, which are more stable when there is a single point of attachment *(14, 15)*. Protein array development during the present study focused on the use of antibodies as the capture ligand. Spacer molecules between the surface and the attached antibody have been shown to increase signal intensity 10-fold *(16)*, but this increase does not guarantee better functionality for all ligand types.

Array technology is a valuable tool for research laboratories but has not been transferred to the high–sample-throughput world of the clinical laboratory. Protein array systems with higher throughput capabilities could supercede current protein immunoassay methods available for key markers. Array systems could enable simultaneous analysis of multiple analytes, miniaturization of assay procedures, reductions in sample and reagent volumes, and more cost-effective determination of markers.

Protein arrays are constructed on the surface of a biochip, and a carrier component transports biochips to different treatment stations within the analyzer. After ligand binding, a chemiluminescent signal is produced, which is measured by a charge-coupled device (CCD)[1] camera and then quantified by imaging software.

Materials and Methods

BIOCHIP SURFACE ACTIVATION TECHNIQUES

Aluminum oxide sheets were pretreated via sonication in a 50 mL/L soap solution at an alkaline pH for 1 h, then washed extensively under sonication with water and acetone. The sheets were then dried overnight under reduced pressure.

After pretreatment, biochips underwent a silanation activation process, and then an additional reaction with a bifunctional linker was performed when dictated by the immobilized biomolecule.

SILANATION TECHNIQUES

3-Glycidoxypropyltrimethoxysilane (GOPTS). After pretreatment, biochips were immersed in a 20 mL/L solution of GOPTS in *o*-xylene containing 2 g/L *N*-ethyldiisopropylamine (DIPEA). The solution was heated at 55 °C for 5 h, and the biochips were allowed to stand in the silane mixture overnight at room temperature. The biochips were washed twice in toluene and once in acetone and placed directly in a desiccator overnight under reduced pressure.

Isocyanatopropyltriethoxysilane (ICPTES). The aluminum oxide sheets were cleaned by sonication in 50 mL/L alkaline detergent solution in deionized water for 1 h, followed by rinsing in deionized water. The sheets were then dried in an oven at 120 °C. The silanation was carried out in 50 mL/L ICPTES in anhydrous toluene containing 10 mL/L base at 50 °C under nitrogen overnight. The slides were then washed twice with toluene and once with acetone and then cured at 120 °C.

3-Aminopropyltriethoxysilane (APTES) + 1,4-phenylenediisothiocyanate. The aluminum oxide sheets were cleaned by sonication in 50 mL/L alkaline detergent solution in deionized water for 1 h, followed by rinsing in deionized water. The slides were then dried in an oven at 120 °C. The silanation was carried out in 20 g/L APTES solution in 1 mmol/L acetic acid for 1 h. The slides were washed several times with doubly distilled water, dried under nitrogen, and cured at 120 °C for 30 min.

Biochips with surface-attached polymers were immersed in a 10 g/L linker solution in acetonitrile containing 10 g/L DIPEA for 6 h at room temperature. The biochips were then washed 3 times in acetonitrile and twice in acetone. The biochips were then dried overnight at 37 °C.

X-RAY PHOTOELECTRON SPECTROSCOPY ANALYSIS

X-ray photoelectron spectroscopy (XPS) analysis was performed with a Surface Science Instruments M-probe spectrometer (operating at a base pressure 3×10^{-9} torr, with the energy scale calibrated using the gold and copper peaks). The samples were irradiated with monochromatic Al Kα x-rays (1486.6 eV), using an x-ray spot size of 1000×400 μm and ~180 W of power. Survey spectra were recorded with a pass energy of 150 eV, from which surface chemical compositions were determined. Appropriate charge compensation was applied. The samples were analyzed predominantly at the standard electron takeoff angle of 35 degrees and a diving maximum analysis depth of 3–5 nm. In addition, when effects related to layer depth were investigated, some measurements were done with a 15-degree takeoff angle to investigate the outermost 1-nm–thick layer of the surface.

A polymer method (PP) technique was also used for surface activation. The details of this method of activation cannot be disclosed because it is a proprietary method.

SECONDARY ION MASS SPECTROMETRY ANALYSIS

Secondary ion mass spectrometry (SIMS) analysis was carried out with a MiniSIMS instrument (Millbrook). A range of biochip surfaces was investigated, including raw and treated (silane- and protein-coated) substrates, which

[1] Nonstandard abbreviations: CCD, charge-coupled device; GOPTS, 3-glycidoxypropyltrimethoxysilane; DIPEA, *N*-ethyldiisopropylamine; ICPTES, isocyanatopropyltriethoxysilane; APTES, 3-aminopropyltriethoxysilane; XPS, x-ray photoelectron spectroscopy; PP, proprietary long polymer; SIMS, secondary ion mass spectrometry; DTR, discrete test region; and RLU, relative light unit(s).

amounted in total to over 250 samples (sample size was that of a typical Randox biochip, 9 × 9 mm) from a representative selection of production batches.

CONTACT-ANGLE MEASUREMENTS

A Cam200 optical contact-angle system (KSV) was used to determine contact-angle measurements of water droplets applied to each biochip surface. Activated and unactivated substrate slides were presented to the measurement platform. Twenty-three water droplets (3.4 μL each) were sequentially added across each slide surface, and the contact angle was measured for each of those droplets. Contact-angle measurements were then calculated as the mean of the 23 measurements.

LIGAND ATTACHMENT AT DISCRETE TEST SITES

A piezoelectric nanodispense technique was used in a humidity-controlled environment under cleanroom conditions; 330-pL droplets were applied sequentially to achieve a total volume of 10 nL of ligand solution, without affecting antibody structure and conformation.

Different ligands were dispensed at predefined *x,y* coordinates on the biochip surface, creating discrete test regions (DTRs), each ~300 μm in diameter. Typically, a 5 × 5 array was manufactured within a 7 × 7 mm biochip area; however, greater densities have been achieved with smaller dispense volumes.

AUTOMATED BLOCKING AND STABILIZATION OF BIOCHIP ARRAYS

After ligand attachment, biochip surfaces were treated at 25 °C with proprietary blocking solutions to eliminate surface reactivity between the DTRs and to reduce nonspecific binding. The arrayed biomolecules immobilized on the biochip were treated further to stabilize the ligands and provide a long-term shelf life of the biochip array.

DETECTION TECHNIQUE

The Evidence system uses enhanced chemiluminescent substrate with a horseradish peroxidase label for the detection of antibodies or analytes bound to the biochip surface. The signal reagent used in the Evidence system contains a 1:1 mixture of luminol/enhancer solution and a peroxide solution.

Light emission from the chemiluminescent reactions at DTRs on the surface of the biochip were detected and quantified by a CCD camera. The CCD camera simultaneously records the light emissions from all discrete test sites on each of the 9 biochips contained in the biochip carrier. A software imaging process is then used to quantify and validate the signal.

BIOCHIP ASSEMBLY

Biochips of dimensions 9 × 9 mm were secured in the base of a plastic well, which was then placed in a carrier holding 9 biochips in a 3 × 3 format, allowing 9 samples to be assayed in each carrier simultaneously (Fig. 6). Each well served as a reaction vessel to contain sample and reagents during the biochip assay. Fabrication of the biochip carrier and reaction well were designed to minimize meniscus effects during imaging. The biochip carriers were then vacuum-sealed in bags.

PERFORMANCE STUDIES

Evidence assay reagents, controls, calibrators, and the Evidence analyzer, all from Randox Laboratories, were used to perform all biochip studies. Intraassay precision was determined from the results of 20 replicates measured within the same run on the analyzer, and interassay precision was determined from the results of 2 replicates of the same samples over 10 separate runs on the analyzer. This procedure was repeated on 3 consecutive days to determine interassay precision. Theoretical sensitivity is the lowest concentration that can be distinguished from 0 (2 SD above 0). The functional sensitivity is the lowest concentration that gave a CV <20% on 20 replicates.

CORRELATION STUDIES

Quantikine ELISAs (R&D Systems) were used for the cytokine comparison studies. Assays were performed according to the manufacturer's specifications in the assay inserts. A total of 57 samples were analyzed for the correlation studies, including Evidence cytokine calibrator samples, R&D Systems calibrator samples, National Institute for Biological Standards and Control reference material samples, and patient samples. All samples were analyzed in duplicate on both systems, and the mean results are presented.

Results

To ensure reproducible fabrication of stable biochips for automated analysis of samples, we assessed many aspects of biochip production, including substrate selection, substrate activation (for attachment of ligands), ligand attachment at spatially separated locations, surface blocking, and stabilization of the biochip.

Aluminum oxide was selected from a variety of possible biochip substrates, and activation techniques involved pretreatment for direct, linker, or long-polymer–ligand attachment to the surface. Before ligand attachment, it was important to ensure that chemical activation of the biochip surface was complete and uniform across the biochip surface.

SIMS AND XPS

SIMS and XPS analytical techniques were used to characterize the different surfaces after activation and to assess uniformity of the surface chemistry across the biochip. XPS yielded information on the atomic composition of the activated surface, whereas SIMS gave information on the molecular fragment species on the surface. Static SIMS was then used to analyze the outermost atomic layers, and depth profiling was performed by sequentially eroding layers of the biochip in the dynamic SIMS mode.

XPS analysis was performed on biochip samples at different stages of "layering", including untreated, pretreated, and silanated substrate. Multiple measurements from different areas on the same sample and on multiple samples confirmed consistent chemical composition of the uncoated solid alumina substrate. The main chemical elements of the untreated substrate were determined to be oxygen, aluminum, silicon, and some impurities including carbon, magnesium, calcium, sodium, phosphorus, sulfur, and nitrogen (Table 1).

After surface silanation was performed with various methods, elements of the silane coatings were quantified as shown in Table 1. The carbon content of the organosilane-coated substrates was notably higher than that of the uncoated substrate, indicating the presence of the coating. Nitrogen was detected, as expected, in 2 of the silane-coated samples, compared with only trace amounts in the uncoated substrate. GOPTS does not contain nitrogen, and nitrogen was not detected on the GOPTS-coated surface. The aluminum content of the uncoated surface was significantly higher than that of the coated surfaces, indicating that the activation processes successfully covered the alumina-based substrate.

Spectral analysis from the carbon 1s spectrum of the GOPTS-coated substrate showed significant oxygen functionality, which was attributed mainly to C−O bonding in the GOPTS molecule. We carried out further analysis of GOPTS silane to confirm surface functionality by attaching 1,9-diaminononane. The attachment was indicated in the XPS spectra by an increase in nitrogen content attributable to the amine and protonated amine species. This result further validates the success of the activation technique, which enabled subsequent attachment of proteins.

SIMS involved bombarding the biochip surface with a high-energy primary ion beam, producing a range of secondary ions, both positive and negative, that were mass-separated and detected. The outermost atomic and/or molecular layers were analyzed (static SIMS), and depth profiling of the chemical composition was studied by eroding the sandwiched layers of the biochip in the dynamic SIMS mode. We also used SIMS to map the elements and molecular fragments on surfaces.

We used SIMS to assess surface chemistry at each stage of the biochip surface activation procedure. A range of biochip surfaces was investigated, including raw and treated substrate and silane- and protein-coated samples from a representative selection of production batches. We verified the success of the silanation procedure by assessing the surface content of various ions, such as CH^-, C_2H^-, $C_2H_5^+$, $C_3H_7^+$, CN^-, and some other species of higher masses characteristic of organic carbon species, compared with the species associated with the unsilanated inorganic substrate.

Silanation of the biochip surface increases the CN^- content, which is displayed as a peak at mass 26 (Fig. 1A). Results show that the pretreated (unactivated) surface had negligible CN^- content, whereas for the PP coating, a large peak at mass 26 indicates significant silanation. This analysis was repeated at many locations across the biochip surface and on samples from different batches to confirm the reliability of the silanation process. These results confirmed that the silanation technique was successful and that the surface had been chemically modified. The CN^- content on the ICPTES-coated substrate was much lower than on the surface prepared by the PP method.

Integrated peak intensity ratios were calculated between several different peaks in the spectrum corresponding to different species as detailed in Table 2. The CN^- peak was selected for ratio determination because it is characteristic of functionality and would be expected in both ICPTES- and PP-silanated surfaces. The results show some CN^- species in the pretreated substrate, indicating a background concentration. Silanated ICPTES and PP substrates have much higher concentrations of CN^- species (higher ratios with base substrate indicators) than the unactivated surface, indicating successful surface alteration.

ICPTES treatment involves linker attachment and is expected to give a single layer after activation, whereas PP treatment involves attachment of a longer polymer, which is expected to generate a thicker layer on the surface. The sequential increase in surface CN^- species from an unactivated surface to the one with attached linker and then to the surface with the long polymer attached, as seen in Table 2, supports the theoretically expected surface chemistry design.

SIMS analysis demonstrated generation of a surface-

Table 1. XPS data from a representative selection of biochip surfaces.[a]

	Concentration, atomic %				
	Carbon	Oxygen	Silicon	Aluminum	Nitrogen
Untreated chip	16	46.1	5.0	30.3	0.3
APTES-coated biochip	47.0	31.6	13.4	2.6	5.4
GOPTS	52.4	34.4	12.2	1.1	
Proprietary polymeric silane + bifunctional aromatic linker	35.3	29.2	5.4	14.7	12.0

[a] The values are based on XPS spectral analysis of the biochip surfaces.

Table 2. SIMS analysis of unsilanated and silanated biochip surfaces.

	Integrated peak intensity ratios		
	Pretreated	ICPTES	PP
CN^- (mass 26): species **1** (organic)[a]	0.3	1.4	7.3
CN^- (26): species **2** (inorganic and/or organic)	3.9	50.7	397.7
CN^- (26): species **3** (organic)	0.1	0.4	4.0
CN^- (26): species **4** (inorganic)	1.0	11.4	153.5

[a] Species shown: **1**, C_2H^- (mass 25); **2**, AlO_2^- or $C_3H_7O^-$ (mass 59), corresponds predominantly to alumina species; **3**, CH^- (mass 13), corresponds to the presence of hydrocarbons on the surface; **4**, SiO_2^- (mass 60), corresponds to the presence of the base substrate.

coating layer, and XPS analysis carried out in addition to SIMS revealed more detailed information on the functional groups exposed on the activated surface.

We used additional XPS analysis to confirm the presence of an aromatic bifunctional linker attached by design to PP substrate. The success of surface activation with a nitrogen-containing aromatic compound was confirmed on the basis of a nitrogen 1s peak binding energy, which indicated that most of the nitrogen present was in the form of a ring compound rather than an amine/amide (Fig. 1B).

A typical depth profile, in which increasing time represents increasing depth, is shown in Fig. 1C. The CN^- coating species disappear as the etching process removes the activated surface layer. After removal of the coating, the substrate species remain reasonably constant.

Depth profiling in the dynamic SIMS mode showed that the coating species gradually disappeared as the top surface layer was etched out until only the base substrate species was identified.

CONTACT-ANGLE MEASUREMENTS

We studied all aspects of ligand attachment to ensure accurate dispensing of ligands to form DTRs, buffer optimization to ensure maintenance of DTRs and biomolecule stability, optimization of spotting techniques, and stability of DTRs and prevention of cross-contamination between DTRs.

To ensure containment of the spotting solution during the ligand attachment process, production of uniform spot shapes, and prevention of spot spreading across the

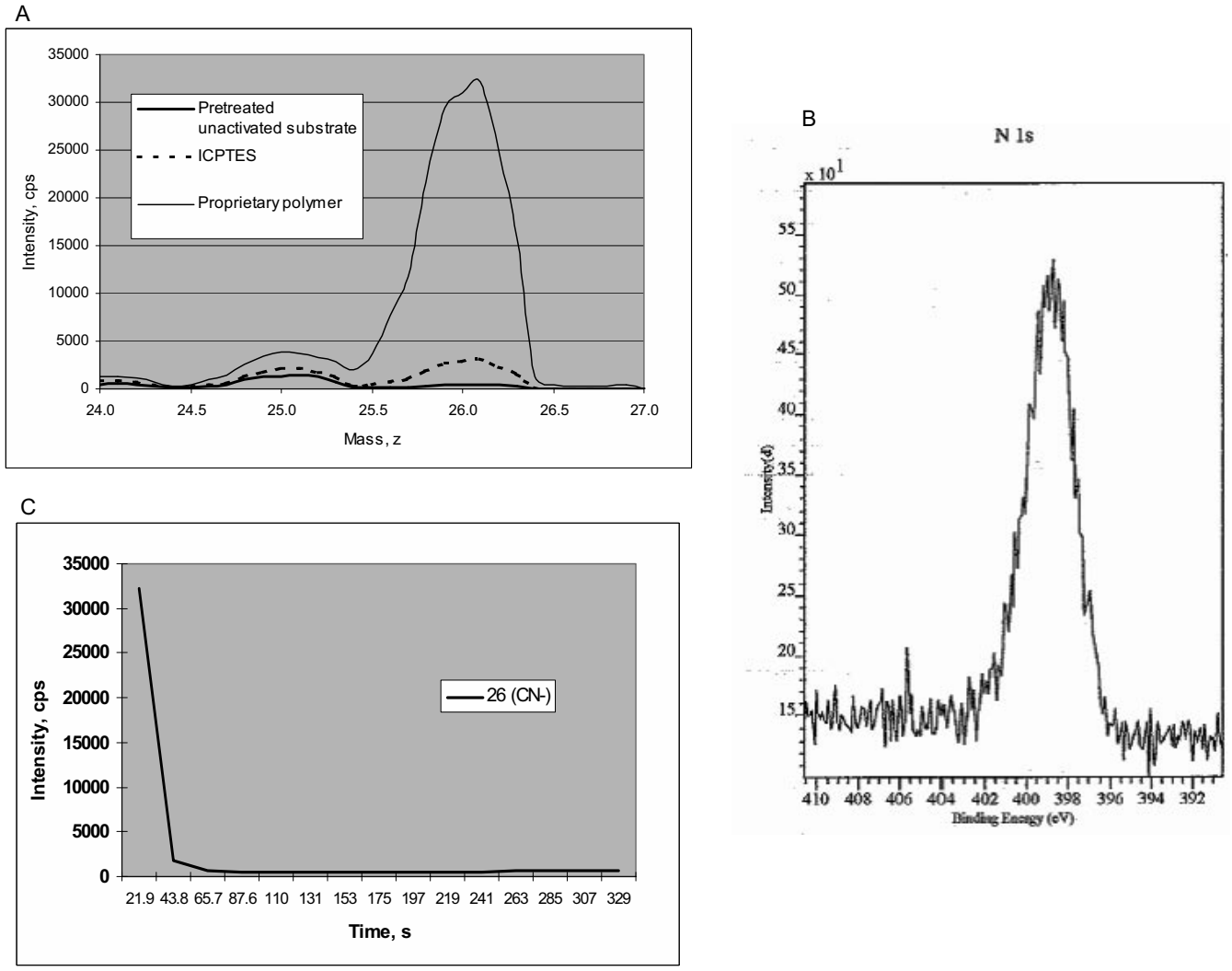

Fig. 1. Results of SIMS, XPS, and negative-ion analysis.

(*A*), SIMS analysis of unsilanated and silanated biochip surfaces. A typical negative ion spectrum measured on a Millbrook MiniSIMS spectrometer (mass range, 24–27; mass step, 0.1; dwell, 0.05; 5 scans) from the sample of pretreated biochip substrate compared with those from 2 samples of silane-coated surfaces. To identify the full range of the species present, SIMS analysis was performed across the full mass spectrum from mass 2 up to mass 150, but for some species of interest, spectra were acquired at higher mass resolution and longer dwell times. Shown is a high-resolution spectrum between masses 24 and 27. (*B*), XPS spectrum of an activated PP substrate with a nitrogen 1s peak. (*C*), example of negative ion depth profile obtained on a PP-coated surface. The data show that CN^- species are concentrated in a thin and easily removable top layer of the surface.

biochip, a hydrophobic surface was deemed desirable. Silanation in addition to introduction of functionality on the surface changes the characteristics of the surface in relation to its ability to repel water, making it more hydrophobic.

We used contact-angle measurement to measure the hydrophobicity of the biochip surface at each stage of the activation process. The greater the contact angle, the more hydrophobic the biochip surface. Fig. 2A shows a droplet of water on an unactivated substrate, demonstrating a low contact-angle measurement with the surface and spreading of the droplet. Fig. 2B shows a droplet of water on an activated substrate, demonstrating that the contact angle has increased because of enhanced hydrophobicity of the substrate. This hydrophobicity prevents spread of the liquid across the biochip surface and ensures retention and preservation of the DTR at the position of application.

The contact angles for a range of activation techniques described in this report are shown in Fig. 2C. The contact angle found in the pretreated unactivated surface was low

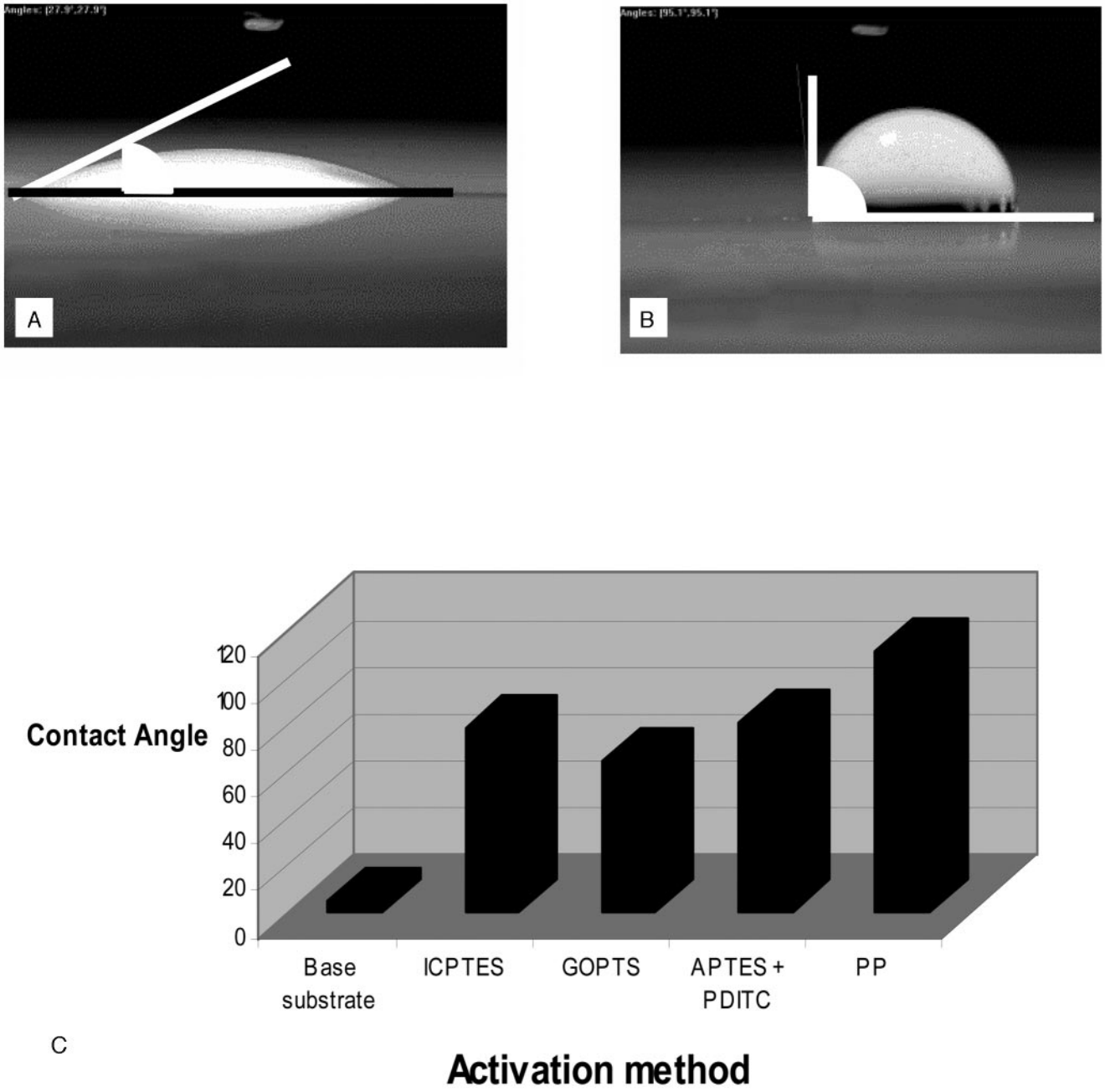

Fig. 2. Contact-angle measurements for unactivated (*A*) and activated surface (*B*), and effect of surface chemistry on contact-angle measurement (*C*).
PDITC, 1,4-phenylenediisothiocyanate.

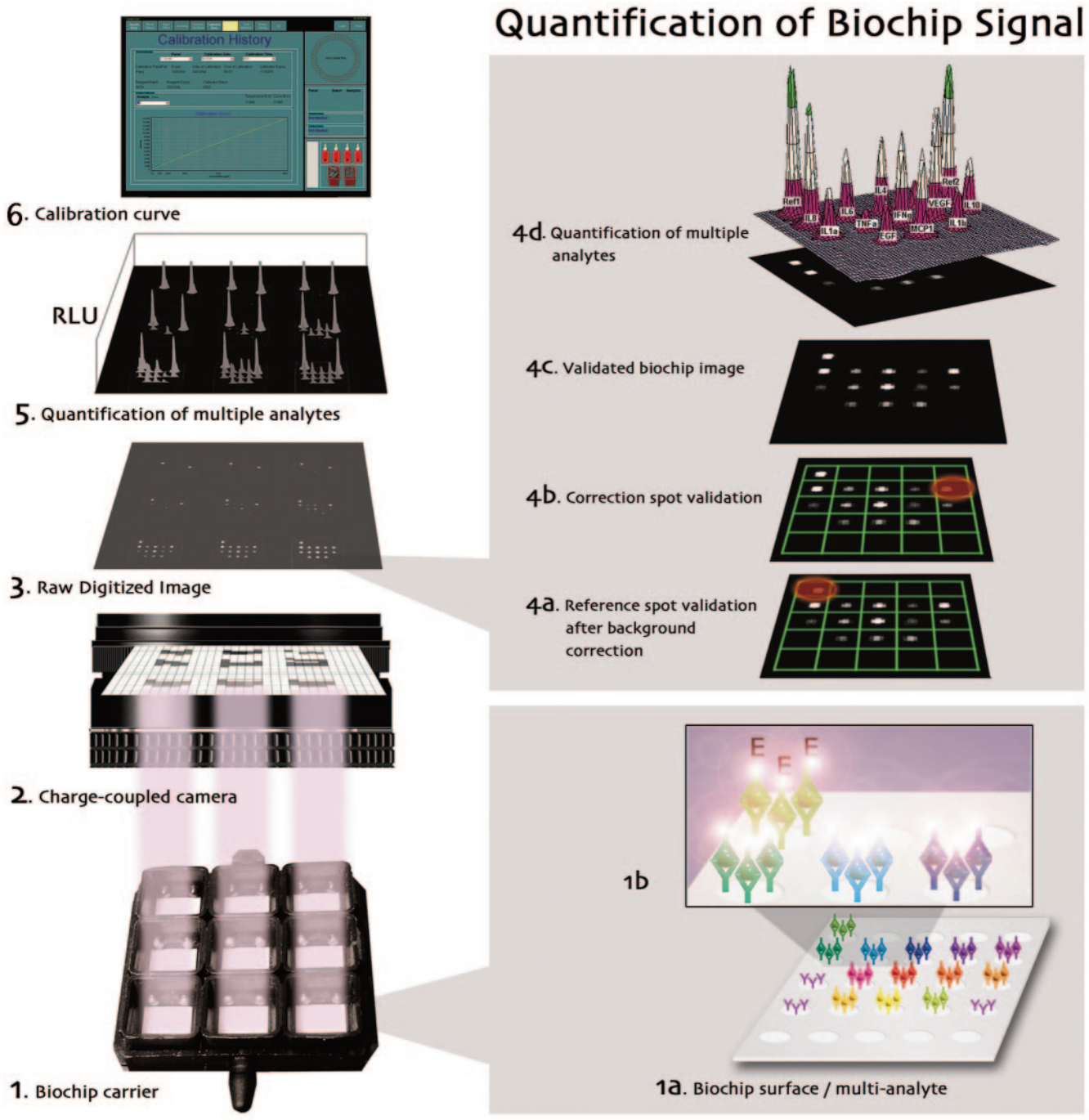

Fig. 3. Evidence procedure for image analysis and quantification of signal from biochips.

(*1*), all Evidence assay steps are carried out automatically in the analyzer. Biochips are presented in a 3 × 3 format in the biochip carrier. (*1a*), DTRs for multiple markers are presented in an ordered array on the biochip surface. (*1b*), when a DTR ligand captures an analyte during the assay, a complex is formed that outputs light after addition of signal reagent. (*2*), light output from the DTRs falls on the photosites within the CCD camera, and the pattern is digitized. (*3*), the raw digitized image is corrected by imaging techniques by subtraction of background signal from the image. (*4a–4d*), validation and quantification of the background-corrected image are carried out simultaneously on each biochip: (*4a*), reference spots are located by the software at predefined *x* and *y* coordinates to validate the biochip; (*4b*), correction spots are then used to define and locate each DTR; (*4c*), a validated biochip image is produced, which undergoes image analysis for quantification of signal at each DTR; (*4d*), an RLU output graph is produced for each DTR. (*5*), quantification of the signal from DTRs in multiple biochips in the 9-well carrier format is performed, and RLU values are quantified for each DTR. (*6*), validated calibration curves are used for each marker to determine the analyte concentration for each DTR in the carrier.

compared with the values typically seen for the activated surfaces, which ranged from ~65 degrees for the GOPTS to a maximum of 111 degrees for the proprietary polymer method.

DETECTION PRINCIPLES

Competitive and sandwich immunoassay techniques were used for biochip assays. Competitive assays used an enzyme-labeled analyte for detection, whereas the sand-

wich assay uses an enzyme-labeled antibody. Details of the detection method are shown in Fig. 3.

EFFECT OF SURFACE ACTIVATION TECHNIQUE ON LIGAND ATTACHMENT AND SIGNAL OUTPUT

Nanodispensation of ligands is a critical step in biochip fabrication as the imaging software requires precise location coordinates for each test spot to enable identification and quantification of the signal at each DTR.

Several biochip activation techniques were assessed during development of each test panel. The data below demonstrate the effect of the surface activation method on the signal output, measured in relative light units (RLUs; arbitrary unit used to quantify signal output from the chemiluminescent reaction) for the cytokine test panel. Two activation surfaces were studied, including the direct ICPTES and the PP method.

Signal output was lowest for the direct ICPTES surface, for all cytokine markers (Fig. 4). The maximum RLU signal was observed for the PP method for all markers and was up to 10-fold higher than the ICPTES method for some. The results demonstrate that surface chemistry affects ligand attachment, analyte binding, and signal output of the biochip array assays. The results show that the PP surface activation method is optimal for the cytokine sandwich assays.

However, similar studies on a biochip array adopting a competitive assay technique for detection of drugs of abuse revealed that the direct GOPTS method produced RLU output in excess of light output with the PP surface (Fig. 5). Our results showed that biochips treated with the direct GOPTS method offer better RLU signal and sensitivity of drug detection at the lowest concentrations than the PP method.

AUTOMATION OF BIOCHIP ARRAY ASSAYS

An analyzer system was developed to enable complete automation of reagent addition, agitated incubation, washing, and detection of test analytes on the biochip array for all test panels. Initially, diluent is added to the reaction well covering the entire surface of the biochip. Subsequent addition of sample and controlled agitation ensure uniformity of the reaction solution and interaction of sample components with all DTRs on the biochip surface.

The analyzer consists of an assembly of individual processing stations interlinked by a horizontal transport module, which transports each biochip carrier (containing 9 biochips) between stations in a predefined order (Fig. 6). The carrier device has 2 protruding section arms on either end, one to enable capture by the mechanical grabbing device for transport between stations and the other to secure the carrier in the station.

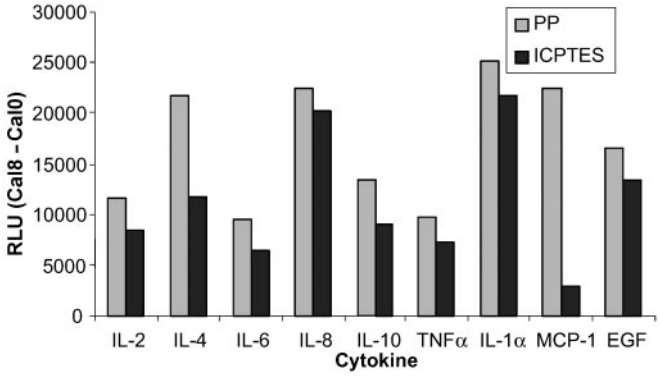

Fig. 4. Effect of surface activation method on the RLU signal [RLU (Cal8 − Cal0)] for the cytokine panel.

The absolute RLU signal is calculated by subtracting the RLU output for the 0 calibrator from the RLU value for the highest calibrator. *IL*, interleukin; *TNFα*, tumor necrosis factor α; *MCP-1*, monocyte chemoattractant protein-1; *EGF*, epidermal growth factor.

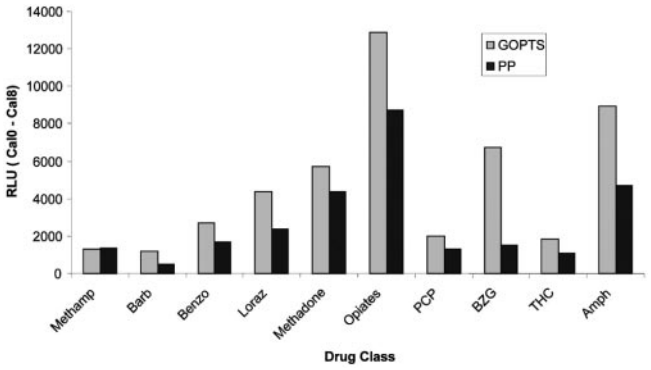

Fig. 5. Effect of surface activation method on the RLU output on the drugs-of-abuse panel.

The absolute RLU signal is calculated by subtracting the RLU output for the highest calibrator from the RLU value for the 0 calibrator. *Methamp*, methamphetamine; *Barb*, barbiturates; *Benzo*, benzodiazepine; *Loraz*, lorazepam; *PCP*, phencyclidine; *BZG*, O^6-benzoylecgonine; *THC*, tetrahydrocannabinol; *Amph*, amphetamine.

VALIDATION OF BIOCHIP PRODUCTION PROCEDURES

Surface chemistry analyses and preliminary manual assays indicated that a hydrophobic surface was produced that enabled ligand attachment for a range of test panels. However, covalent protein attachment to a solid surface is notoriously difficult; we therefore confirmed protein in-

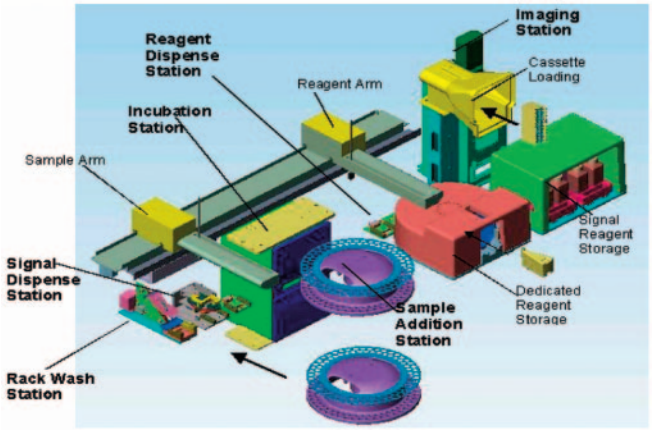

Fig. 6. Evidence biochip array analyzer.

tegrity and activity for different assay panels. Our analysis of instrument performance involved assaying calibrators, controls, and patient samples with different assay panels. The performance information is presented for cytokine results obtained by use of the automated analyzer.

PRECISION DATA AND CALIBRATION CURVES

Precision data. Intra- and interassay precision data for the cytokine test panel are presented in Table 3. Intra- and interassay CVs for most cytokine markers were ≤10% for the fully automated biochip array analyzer.

Correlation data. Correlation studies (n = 57) were performed to compare Evidence results with commercial ELISAs. ELISAs were performed manually, whereas biochip analysis was completely automated, with minimal operator intervention. Results obtained by the Evidence showed good correlation for cytokine markers with the commercial cytokine ELISAs, with correlation coefficients of 0.95–0.99 (Fig. 7).

Calibration curves. Each biochip accommodates multiple reaction sites, each site specific for a particular analyte. A single biochip carrier containing 9 biochips was sufficient to perform a 9-point calibration for each of the cytokine markers simultaneously. A multianalyte calibrator was added to each biochip and then processed in the same way as a sample.

Calibration curves for all markers in each of the test panels are shown in Fig. 8. All cytokine assays are based on sandwich techniques and demonstrate a sequential increase in signal output with increasing concentration of analyte. These results demonstrate the accuracy of DTR location, the quantity of ligand applied, and the ability of the analyzer to simultaneously detect and quantify different concentrations of analytes in samples.

Discussion

Biochip array technology is applicable to the detection of a wide range of substances and offers benefits to all areas of scientific investigation. Microarray systems, however, are perceived to be in their infancy. Existing panels are

Table 3. Performance of the range of cytokine markers on the Evidence cytokine panel.

	Sensitivity,[a] ng/L			Intraassay precision (n = 20)		Interassay precision (n = 20)	
Analyte	Theoretical	Functional	Range, ng/L	Mean, ng/L	CV, %	Mean, ng/L	CV, %
IL-2[b]	5.1	11.5	11.5–1000	20.3	10	39.9	9.6
				82.0	5.5	155.9	8.1
				322.0	5.6	625.8	5.4
IL-4	0.4	5.3	5.3–1000	17.0	6.8	26.9	12
				42.0	6.6	110.8	9.7
				130.0	4.9	367.6	9.0
IL-6	0.2	1.1	1.1–350	3.9	7.8	9.28	6.5
				13.8	5.8	33.3	7.4
				49.8	7.8	140.5	6.2
IL-8	1.5	8.9	8.9–2000	14.8	11	32.97	11
				66.0	6.6	130.3	6.8
				258.0	6.3	526.7	10
IL-10	1.6	1.8	1.8–600	6.4	4.4	14.7	6.5
				28.0	6.1	60.7	6.4
				113.0	6.5	256.99	6.9
TNFα	0.6	7.7	7.7–1000	11.5	7.3	22.1	12
				45.0	5.6	84.3	7.9
				167.0	4.8	324.8	8.5
IL-1α	0.4	3.6	3.6–500	11.5	5.3	12.8	7.2
				45.0	3.9	47.2	5.8
				172.0	4.2	202.6	7.5
IL-1β	1.3	1.7	1.7–500	3.0	8.2	13.6	9.8
				9.8	4.5	52.5	10
				38.0	4.3	228.8	7.9
MCP-1	3.0	12.3	12.3–1200	45.0	8.4	72.2	8.9
				144.0	6.0	280.6	6.5
				408.0	7.7	543.2	4.2
EGF	1.0	1.8	1.8–500	7.4	10	13.2	13
				27.0	7.1	59.5	8.6
				101.0	5.6	246.9	7.2

[a] See text for definitions.

[b] IL, interleukin; TNFα, tumor necrosis factor-α; MCP-1, monocyte chemoattractant protein-1; EGF, epidermal growth factor.

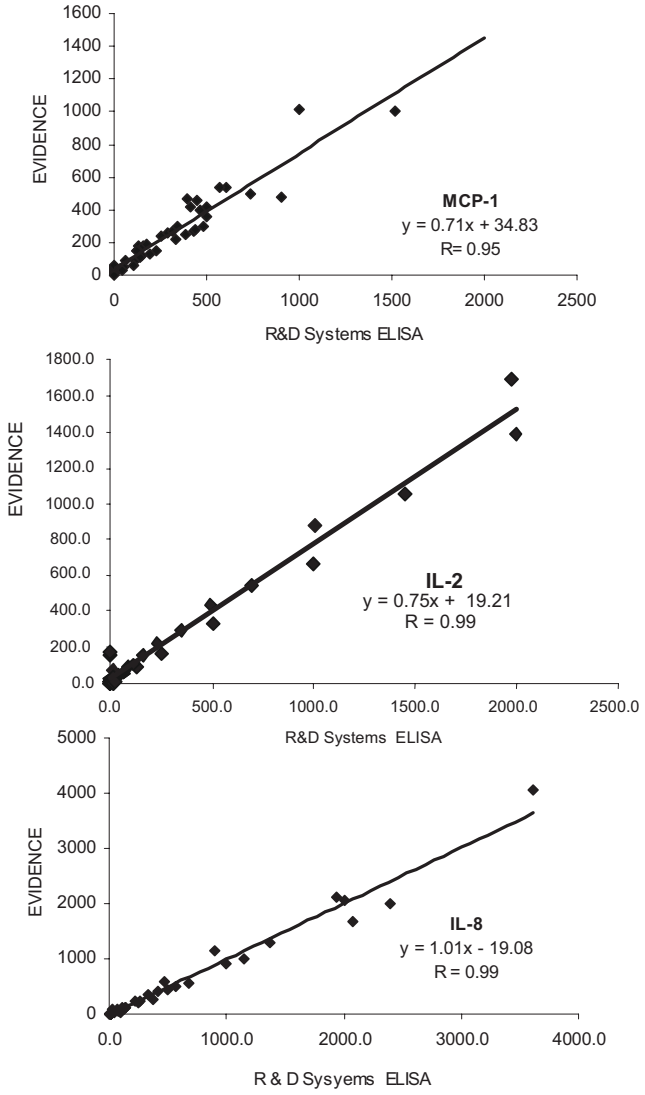

Fig. 7. Samples (n = 57) assayed for correlation studies.

Samples include Evidence calibrators, R&D Systems ELISA calibrators, National Institute for Biological Standards and Control reference material, and 21 patient samples. Results (ng/L) were compared for Evidence cytokine assays and R&D Systems ELISAs. *MCP-1*, monocyte chemoattractant protein-1; *IL*, interleukin.

based on low-density arrays to meet current needs in the clinical diagnostic market, but these systems have much more diverse technological potential, with spotting procedures developed for up to 100 different capture molecules on the surface of a biochip.

Many challenges and obstacles exist for fabrication of protein arrays on a solid surface and stabilization and reproducibility of biochip performance in patient samples. The novel procedures described here enabled successful biochip fabrication and precise ligand attachment at multiple DTRs for test panels. The stable calibration curves and excellent precision data demonstrate the accuracy and reproducibility of the image-processing and detection methods used. The introduction of the Evidence analyzer enabled complete automation of assays for test output volumes of up to 2000 results per hour.

Direct ligand attachment to the biochip surface appears optimal for competitive assays, which are generally used for the detection of low–molecular-weight analytes. This less complex surface may offer better accessibility for the competing analytes and more sensitive detection at the lowest concentrations. However, ligand attachment using a long polymer appears optimal for sandwich assays, which are generally used for detection of high–molecular-weight analytes. This more complex attachment may reduce nonspecific binding and hold analytes away from the biochip surface, enabling ease of interaction.

Biochip activation procedures varied for each of the different test panels supported by this system. In-depth analysis of surface chemistry, surface reactivity, and more importantly, signal output is required before an activation method can be selected for a particular test panel. Our studies have shown that a surface activation technique optimal for one panel may not be the optimal for another panel. This variation is probably attributable to the structural and chemical intricacies of different biomarkers on each of the test panels.

All of our modification techniques produced hydrophobic surfaces *(15)*, which prevent spread and enable containment of the ligand solution on the biochip surface. This strategy is in contrast to other published protein array techniques that use hydrophilic surfaces *(17)*.

The benefits of using a panel approach to sample analysis include a reduction in sample volume per test and simultaneous testing of all analytes, giving a snapshot of a patient's status at a single point in time. This approach provides more diagnostic evidence on the patient, offering a more holistic approach to sample analysis and, potentially, a more accurate diagnosis. Laboratory budgets and cost per test are issues for all busy laboratories. This system reports only results for user-selected tests and offers a unique reporting facility with retrospective access to all test results.

Cost containment of biochip manufacturing processes and upscaling to commercial production are challenging because the fabrication process requires controlled conditions of temperature and relative humidity to ensure consistency of surface chemistry reactions and prevent contamination by air-borne particles. We used robotic systems to minimize human handling and prevent contamination of surfaces. An automated vision system detected deviations in spot size, shape, and positioning in the array, ensuring that all biochips met the necessary analytical requirements. All manufacturing processes, from fabrication to packaging, were carried out within a controlled cleanroom environment to ensure process consistency in a biochip manufacturing facility with a production capacity of >20 million biochips per year. More than 2 million biochips were manufactured in the commercial production facility in the first year of production.

A multitasking approach was integral to the smooth operation of the automated, high-throughput analyzer.

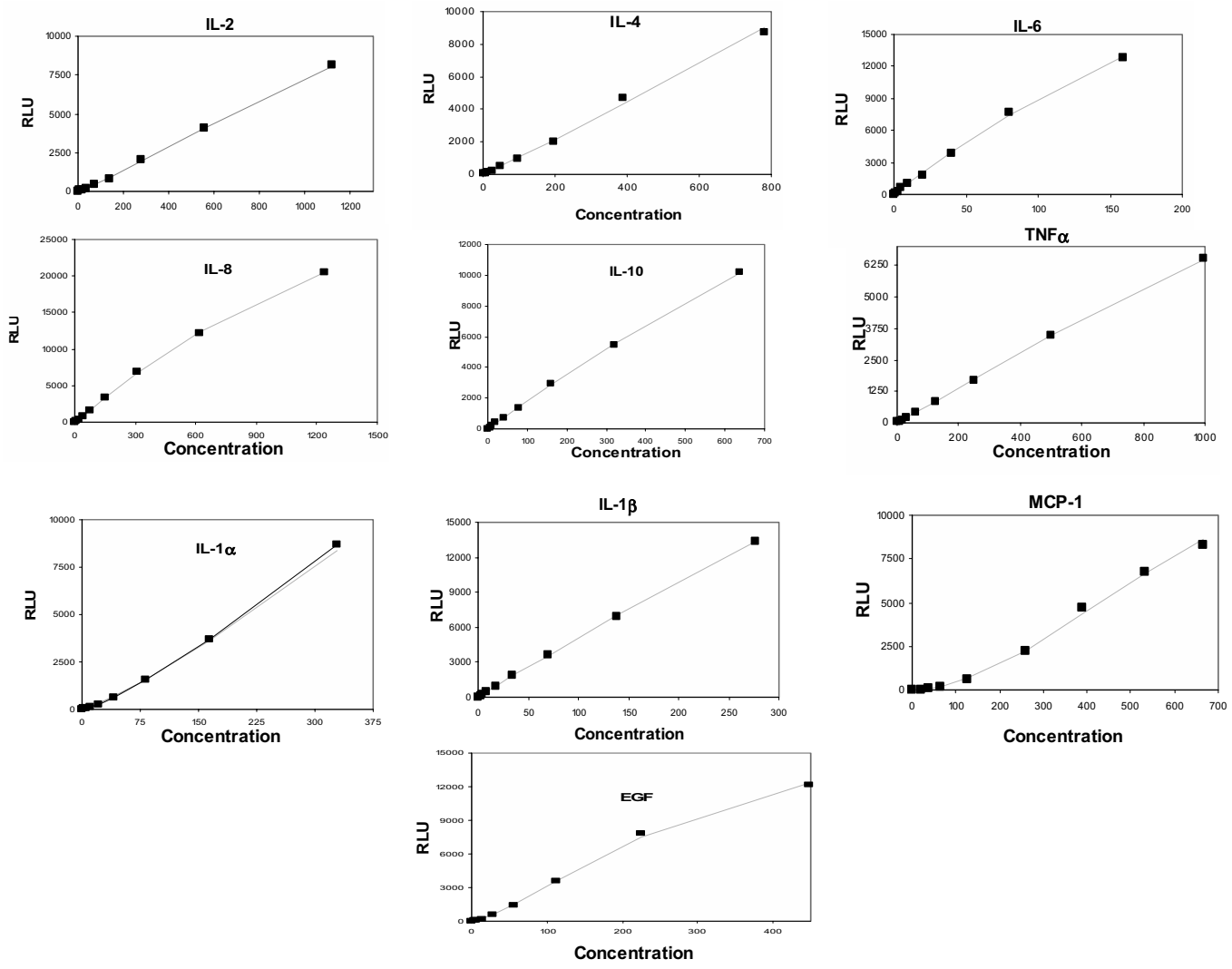

Fig. 8. Calibration curves generated for the 10 cytokine markers.

Nine concentrations (in ng/L) of multianalyte calibrator samples were added to biochips, and the calibration curves were constructed from the results of a single biochip carrier (9 biochips). *IL*, interleukin; *TNFα*, tumor necrosis factor α; *MCP-1*, monocyte chemoattractant protein-1; *EGF*, epidermal growth factor.

Complex image-processing techniques with an output capacity in excess of 2000 test results and light signals quantified every hour enabled simultaneous quantification of light signals from multiple DTRs on each biochip surface. Our dedicated software rapidly processed and quantified the multitude of data for automatic DTR identification and validation procedures during analysis. Unique analyzer control checks incorporated in the software ensure efficient sample processing and accuracy of results.

Ongoing research is set to develop the system capabilities further with applications suitable for use in protein profiling to accelerate the identification of drug targets and disease markers. Multianalyte testing has applications in many areas, including endocrinology, where results for several different markers are required for elucidation of a diagnostic condition. Other areas of application include screening of transfused blood for infectious diseases, inflammatory conditions, and DNA analysis. The availability of this automated system to measure large numbers of analytes simultaneously with excellent sensitivity for a variety of sample types is set to dramatically change diagnostic testing.

References

1. Mazzola L. Commercialising biotechnology. Nat Biotechnol 2003; 21:1137–43.
2. Kricka LJ, Joos T, Fortina P. Protein microarrays: a literature survey. Clin Chem 2003;49:2109.
3. Moody MD, Van Arsedell SW, Murphy KP, Orencole SF, Burns C. Array based ELISAs for high throughput analysis of human cytokines. Biotechniques 2001;31:186–90.
4. Robinson WH, DiGenerro C, Hueber W, Haab BB, Kamachi M, Dean EJ, et al. Autoantigen microarray for multiplex characterization of autoantibody responses. Nat Med 2002;8:295–301.

5. Ekins R. Measurement of free hormones in blood. Endocrinol Rev 1990;11:5–46.
6. Ekins R, Chu F, Biggart E. Multispot, multianalyte immunoassay. Ann Biol Clin 1990;48:655–66.
7. Ekins RP. Ligand assays: from electrophoresis to miniaturized microarrays. Clin Chem 1998;44:2015–30.
8. Mendoza LG, Mc Quarry P, Mongan A, Gangadharan R, Brignac S, Eggers M. High throughput microarray based enzyme linked immunosorbent assay (ELISA). Biotechniques 1999;27:778–88.
9. Kusnezow W, Jacob A, Walijew A, Diehl F, Hoheisel JD. Antibody microarrays: analysis of production parameters. Proteomics 2003;3:254–64.
10. Jonsson U, Malmqvist M, Ronnberg I. Immobilisation of immunoglobulins on silica surfaces stability. Biochem J 1985;227:363–71.
11. Lin JN, Andrade JD, Chang IN. The influence of adsorption of native and modified antibodies on their activity. J Immunol Methods 1989;125:67–77.
12. Polzius R, Schneider T, Biert FF, Bilitewski U, Koschinski W. Optimisation of biosensing using grating couplers: immobilisation on tantalum oxide waveguides. Biosens Bioelectron 1996;11:503–11.
13. Kusnezow W, Hoheisel JD. Solid supports for microarray immunoassays. J Mol Recognit 2003;16:165–76.
14. Wilchek M, Miron T. Oriented versus random protein immobilisation. J Biochem Biophys Methods 2003;55:67–70.
15. Danczyk R, Kreider B, North A, Webster T, HogenEsch H, Rundell A. Comparison of antibody functionality using different immobilisation methods. Biotechnol Bioeng 2003;84:215–23.
16. Peluso J, Wilson DS, Do D, Tran H, Venkatasubbaiah M, Quincy D, et al. Optimising antibody immobilisation strategies for the construction of protein microarrays. Anal Biochem 2003;312:113–24.
17. FitzGerald SP, Lamont JV, Mc Connell RI, Benchikh EO, inventors. Method for making a device for the simultaneous detection of multiple analytes. US patent 6,498,010, December 24, 2002.